Structure of the human κ-opioid receptor in complex with JDTic

Huixian Wu[1], Daniel Wacker[1], Mauro Mileni[1], Vsevolod Katritch[1], Gye Won Han[1], Eyal Vardy[2], Wei Liu[1], Aaron A. Thompson[1], Xi-Ping Huang[2], F. Ivy Carroll[3], S. Wayne Mascarella[3], Richard B. Westkaemper[4], Philip D. Mosier[4], Bryan L. Roth[2], Vadim Cherezov[1] & Raymond C. Stevens[1]

Opioid receptors mediate the actions of endogenous and exogenous opioids on many physiological processes, including the regulation of pain, respiratory drive, mood, and—in the case of κ-opioid receptor (κ-OR)—dysphoria and psychotomimesis. Here we report the crystal structure of the human κ-OR in complex with the selective antagonist JDTic, arranged in parallel dimers, at 2.9 Å resolution. The structure reveals important features of the ligand-binding pocket that contribute to the high affinity and subtype selectivity of JDTic for the human κ-OR. Modelling of other important κ-OR-selective ligands, including the morphinan-derived antagonists norbinaltorphimine and 5′-guanidinonaltrindole, and the diterpene agonist salvinorin A analogue RB-64, reveals both common and distinct features for binding these diverse chemotypes. Analysis of site-directed mutagenesis and ligand structure–activity relationships confirms the interactions observed in the crystal structure, thereby providing a molecular explanation for κ-OR subtype selectivity, and essential insights for the design of compounds with new pharmacological properties targeting the human κ-OR.

The four opioid receptors, μ, δ, κ and the nociceptin/orphanin FQ peptide receptor, belong to the class A (rhodopsin-like) γ subfamily of G-protein-coupled receptors (GPCRs)[1] with a common seven-transmembrane helical architecture, and are coupled predominantly to heterotrimeric G_i/G_o proteins. Activation of these receptors by endogenous or exogenous ligands is linked to a number of neuropsychiatric sequelae, including analgesia, sedation, depression, dysphoria and euphoria[2]. The three closely related subtypes, μ-OR, δ-OR and κ-OR, share ~70% sequence identity in their seven transmembrane helices (I–VII), with more variations in the extracellular loops (ECLs) and very little similarity in their amino and carboxy termini[2]. The majority of endogenous opioid peptides have a defined preference for specific subtypes, for example, endorphins act via δ-ORs and μ-ORs, whereas dynorphins preferentially activate κ-ORs. However, most exogenous and synthetic opioid ligands interact promiscuously (see the K_i Database; http://pdsp.med.unc.edu/pdsp.php), probably owing to the high degree of similarity among binding pockets of opioid receptors. Although decades of focused medicinal chemistry efforts have yielded reasonably selective ligands for all four ORs (see the K_i Database), there remains substantial interest in the development of subtype-selective agonists and antagonists.

Recent breakthroughs in elucidating high-resolution structures of GPCRs in complex with small-molecule[3–7] and peptide[8] ligands are providing details of their function[9], leading to numerous rational ligand discovery studies[10,11]. However, whereas most of these structures belong to the α subfamily of class A GPCRs[1], the highly diverse peptide-binding γ subfamily is represented only by the CXCR4 chemokine receptor[8]; additional structural coverage is needed to elucidate the repertoire of features[12] that define the pharmacological profile of this subfamily. The κ-OR, identified based on studies with the κ-type prototypic agonist ketocyclazocine[13], represents an attractive target for structure determination. Several κ-OR-selective partial agonists and antagonists have been developed as potential antidepressants, anxiolytics and anti-addiction medications[14], whereas a widely abused, naturally occurring hallucinogen—salvinorin A (SalA)—was also found to be a highly selective κ-OR agonist[15]. Although many κ-OR agonists and antagonists have not demonstrated desirable pharmacological properties, lacking specificity or displaying frank psychotomimetic actions in humans[14,16], some have been shown to be viable drug candidates. A κ-OR ligand in early stages of clinical development, JDTic (3*R*)-1,2,3,4-tetrahydro-7-hydroxy-N-[(1*S*)-1-[[(3*R*,4*R*)-4-(3-hydroxyphenyl)-3,4-dimethyl-1-piperidinyl]methyl]-2-methylpropyl]-3-isoquinolinecarboxamide), was originally designed as a novel selective κ-OR antagonist[17] that blocks the κ-OR agonist U50,488-induced antinociception, while not antagonizing μ-OR agonist-induced analgesia[18]. JDTic also displays robust activity in rodent models of depression, anxiety, stress-induced cocaine relapse, and nicotine withdrawal[18,19]. Here we report the crystal structure of a human κ-OR construct, κ-OR–T4 lysozyme (T4L), in complex with JDTic at 2.9 Å resolution. The results provide structural insights into the atomic details of molecular recognition and subtype selectivity of the κ-OR and related ORs, and should catalyse the structure-based design of advanced human κ-OR agonists and antagonists with improved pharmacological profiles and enhanced therapeutic efficacies.

Overall architecture of the κ-OR

Structural studies were carried out using an engineered human κ-OR construct (see Methods and Supplementary Fig. 1) and crystallized in cholesterol-doped monoolein lipidic cubic mesophase (see Methods). The construct used showed pharmacological behaviour similar to that of a native receptor expressed in HEK293T cells (Supplementary Tables 2 and 3). Data collection and refinement statistics are shown in Supplementary Table 1.

The structure of κ-OR–JDTic was determined at 2.9 Å in the $P2_12_12_1$ space group. The asymmetric unit consists of two receptors forming a parallel dimer (Fig. 1a). The dimer interface with ~1,100 $Å^2$

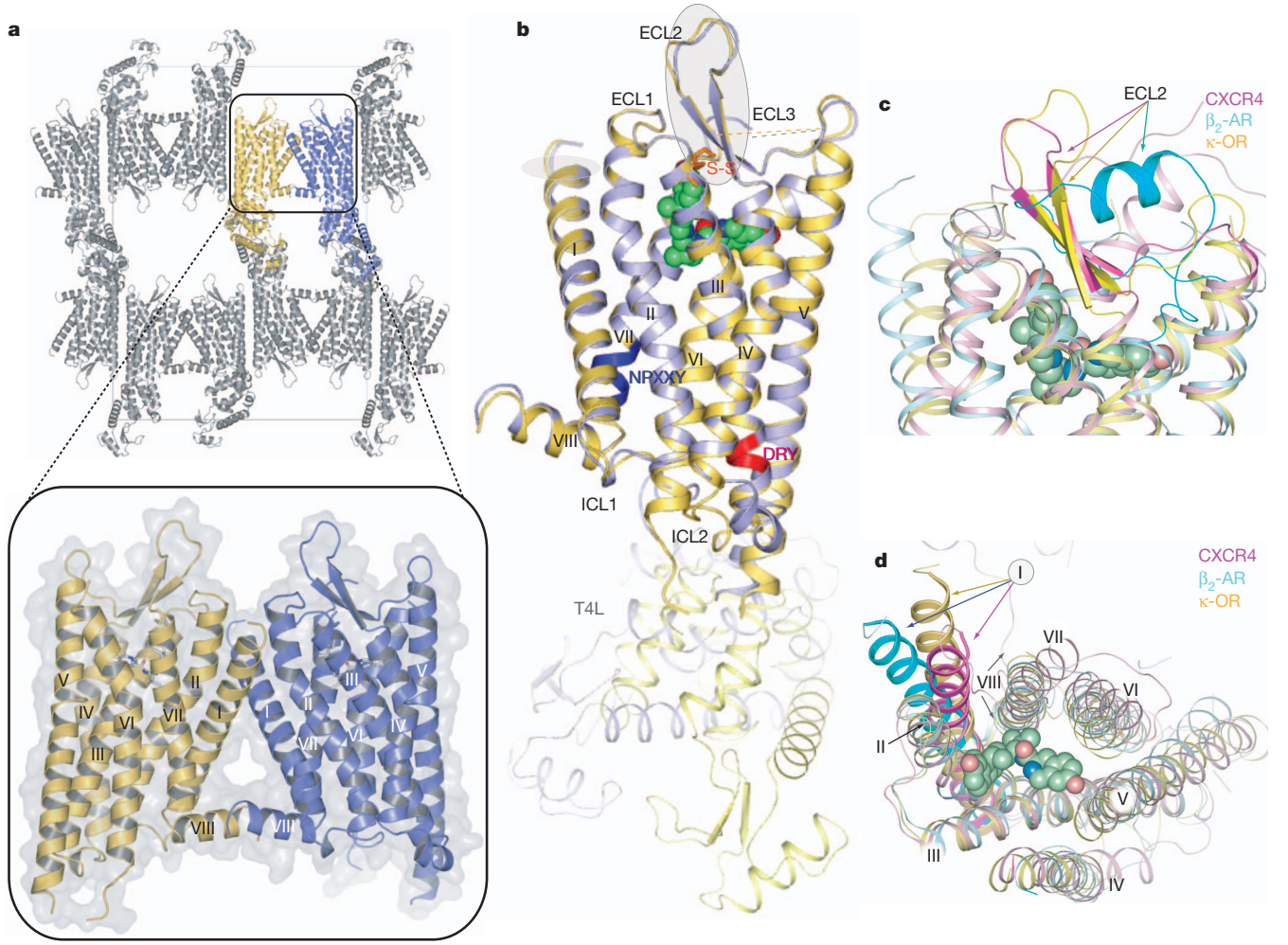

Figure 1 | Crystal packing and overview of the human κ-OR structure in complex with JDTic, and comparison with the inactive CXCR4 and β_2-AR structures. **a**, κ-OR–T4L crystal packing. The parallel dimer in one asymmetric unit is highlighted by the insert. **b**, Overall architecture of κ-OR–T4L in complex with JDTic. The A molecule (yellow) and B molecule (blue) from one asymmetric unit are aligned through the receptor part. The DRY and NPXXY motifs are highlighted in red and blue, respectively. JDTic is shown in a green sphere representation and the disulphide bond is coloured orange. **c**, **d**, Side (**c**) and extracellular (**d**) views of a structural alignment of the human κ-OR (yellow); CXCR4 (PDB accession 3ODU; magenta) and β_2-AR (PDB accession 2RH1; cyan). The graphics were created by PyMOL.

buried surface area is formed through contacts among helices I, II and VIII (Fig. 1a, insert). Previously, parallel receptor dimers have been identified in crystal structures of activated rhodopsin (involving helices I, II and VIII)[20], the β_2 adrenergic receptor (β_2-AR; cholesterol mediated)[3] and CXCR4 (involving helices IV, V and VI)[8]. Consistent with these crystallographic data, recent biochemical studies have suggested the existence of two dimerization interfaces: along helices IV and V (sensitive to receptor activation) and along helix I (insensitive to the state of activation)[21]. Although the orientations of the two T4L copies in the receptor monomers in one asymmetric unit differ by ~60° rotation, both copies of the receptor are highly similar (Fig. 1b) and will be treated identically except where otherwise noted.

The main fold of the human κ-OR consists of a canonical seven-transmembrane bundle of α-helices followed by an intracellular helix VIII that runs parallel to the membrane (Fig. 1a, b), resembling previously solved GPCR structures[3–8]. Structural comparison with other GPCRs suggests that human κ-OR has marked similarities in the ECL region with CXCR4, another peptide-binding receptor in the γ subfamily. In the seven-transmembrane region, however, the κ-OR structure is closer to aminergic receptors belonging to the α subfamily (alpha carbon root mean squared deviation (r.m.s.d.) ~2.3 Å for the β_2-AR, ~1.9 Å for the dopamine D3 receptor (D3R) and ~2.7 Å for CXCR4). The structure reveals distinctive features of the human κ-OR, including the following. First, conformation of the extracellular end of helix I deviates from the position observed in CXCR4, where the tip of helix I is pulled towards the transmembrane bundle by a disulphide bond between the N terminus and ECL3. Second, ECL2, the largest extracellular loop of the human κ-OR, forms a β-hairpin similar to that observed in CXCR4, despite the low sequence similarity in this domain between the two receptors. Conservation of this feature between these peptide receptors suggests that the β-hairpin could be a common motif in the ECL2 of other γ subfamily receptors, where interactions between ECL2 and their endogenous peptide ligands are deemed important for ligand recognition and selectivity[22]. Third, unlike other solved non-rhodopsin class A GPCRs that have more than one disulphide bond, the human κ-OR has only one formed between Cys 131$^{3.25}$ (superscripts indicate residue numbering using the Ballesteros–Weinstein nomenclature[23]) and Cys 210, bridging ECL2 to the end of helix III. These two cysteines are conserved in all opioid receptors and this disulphide bond is the canonical one shared by most other solved class A GPCRs. Fourth, intracellular loop 2 (ICL2) adopts slightly different structures in the two κ-OR molecules in the asymmetric unit, involving a two-turn α-helix in molecule B, and only a one-turn α-helix in molecule A (Supplementary Fig. 2), possibly reflecting the conformational plasticity of this region[5]. Last, ECL3 of the κ-OR is disordered. Of the approximately 11 residues in this loop (residues 300–310), 6 residues in molecule A and 3 in molecule B do not have interpretable electron density.

A common feature of the class A GPCRs is the presence of a conserved sequence motif Asp/Glu$^{3.49}$-Arg$^{3.50}$-Tyr$^{3.51}$ (D/ERY) located at the cytoplasmic end of helix III. A salt bridge interaction between Arg$^{3.50}$ and Asp/Glu$^{6.30}$ from the cytoplasmic end of helix VI constitutes an 'ionic lock', which is thought to stabilize the inactive conformation of rhodopsin and other rhodopsin-like class A GPCRs[5,24], whereas its absence can enhance constitutive activity[6,23]. Although the human κ-OR lacks either of the acidic residues Asp/Glu at position 6.30, Arg 156$^{3.50}$ forms a hydrogen bond to another helix VI residue, Thr 273$^{6.34}$ (Supplementary Fig. 3a) in this inactive κ-OR structure, thereby conceivably stabilizing the inactive receptor conformation. The NPXXY motif located at the cytoplasmic side of helix VII, which is composed of Asn 326$^{7.49}$, Pro 327$^{7.50}$, Ile 328$^{7.51}$, Leu 329$^{7.52}$ and Tyr 330$^{7.53}$ in the κ-OR, is another highly conserved functional motif that is proposed to act as one of the molecular switches responsible for class A GPCR activation[25,26]. Comparison of the human κ-OR with inactive β_2-AR and A_{2A} adenosine receptor (A_{2A}AR) structures (Supplementary Fig. 3b) reveals a similar conformation of this motif in these receptors, thereby supporting the hypothesis that the observed κ-OR–JDTic complex structure corresponds to the inactive state. To establish further that JDTic stabilizes an inactive conformation, we evaluated its ability to modulate G_i/G_o-mediated and β-arrestin-mediated signalling in transfected HEK293T cells. We found that JDTic was devoid of agonist activity at both canonical and non-canonical pathways and completely blocked the effects of the prototypic agonist U69593 (Supplementary Fig. 4).

The κ-OR ligand-binding pocket

The κ-OR ligand-binding pocket displays a unique combination of key characteristics both shared with and distinct from those in the chemokine and aminergic receptor families. Although the human κ-OR binding pocket is comparatively large and partially capped by the ECL2 β-hairpin, as in CXCR4, it is also much narrower and deeper than in CXCR4 (Fig. 2c, d and Supplementary Fig. 5). In addition to a different set of side chains lining the pocket, the shape differences result from an approximately 4.5 Å inward shift of the extracellular tip of helix VI in the κ-OR as compared to CXCR4. The electron density clearly shows the position of the JDTic ligand (Supplementary Fig. 6), which reaches deep into the pocket to form ionic interactions with the Asp 138$^{3.32}$ side chain (Fig. 2a). The Asp$^{3.32}$ residue is conserved in all aminergic GPCRs, thereby having a critical role in the selectivity of aminergic receptors towards protonated amine-containing ligands. Likewise, Asp$^{3.32}$ is conserved in all opioid receptors, and modelling and mutagenesis studies[27] suggest that it has an essential role in anchoring positively charged κ-OR ligands.

Structural basis of JDTic selectivity

JDTic, developed as a derivative of the *trans*-(3*R*,4*R*)-4-(3-hydroxyphenyl)-3,4-dimethyl-1-piperidine scaffold[17], has exceptionally high affinity ($K_i = 0.32$ nM), potency ($K_i = 0.02$ nM in GTPγS assays)[17,28], long duration of action and a more than 1,000-fold selectivity for the human κ-OR as compared to other opioid receptor subtypes[28]. Extensive structure–activity relationship (SAR) analyses performed on JDTic analogues have yielded important insights into key determinants of JDTic activity[28–30], although reliable identification of the interaction mode(s) and contact residues of these ligands has not been feasible without a receptor crystal structure.

The crystal structure of κ-OR–JDTic shows a tight fit of the ligand in the bottom of the binding cleft (Fig. 2a), forming ionic, polar and extensive hydrophobic interactions with the receptor (Fig. 2b). The protonated amines in both piperidine and isoquinoline moieties of the ligand form salt bridges to the Asp 138$^{3.32}$ side chain (3.0 and 2.8 Å nitrogen–oxygen for molecule A, and 2.7 and 2.3 Å for molecule B, respectively). The piperidine amine is part of the original *trans*-(3*R*,4*R*)-dimethyl-4-(3-hydroxyphenyl)piperidine scaffold and is essential for opioid receptor antagonist activity[31]. SAR studies of JDTic analogues show that the isoquinoline nitrogen can be replaced by carbon, oxygen or sulphur atoms with only a ~10- to 50-fold

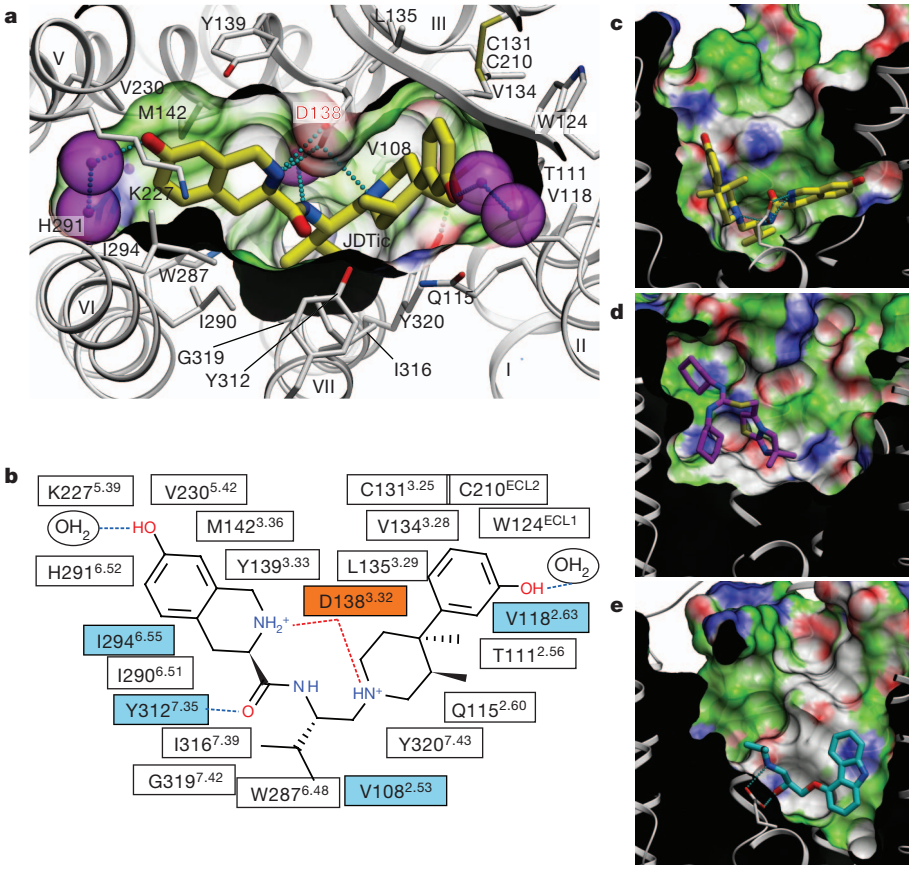

Figure 2 | Binding of the high-affinity selective antagonist JDTic in the human κ-OR crystal structure. **a**, Conformation of the binding pocket with JDTic shown by sticks with yellow carbons. The protein is displayed in cartoon representation looking down from the extracellular side, with the 22 contact residues within 4.5 Å from the ligand shown by white sticks. The pocket surface is shown as a semitransparent surface coloured according to binding properties (green: hydrophobic; blue: hydrogen-bond donor; red: hydrogen-bond acceptor). Salt bridges and hydrogen bonds are shown as dotted lines. Structured water molecules are shown as large magenta spheres. **b**, Diagram of ligand interactions in the binding pocket side chains at 4.5 Å cut-off. Salt bridges are shown in red and direct hydrogen bonds in blue dashed lines. Ballesteros–Weinstein numbering is shown as superscript. Residues that vary among the μ-OR, δ-OR and κ-OR subtypes are highlighted in cyan, and residue Asp 138$^{3.32}$ implicated in κ-OR-ligand binding by mutagenesis data, is highlighted orange. **c**–**e**, Side views of the sliced binding pocket in κ-OR–JDTic (**c**), CXCR4–IT1t (**d**) and β_2-AR–carazolol (**e**) complexes. The pocket surfaces are coloured as in panel **a**, the protein interior is black and the extracellular space is white. Ligands are shown as capped sticks with carbons coloured yellow (JDTic), magenta (IT1t) and cyan (carazolol). Asp$^{3.32}$ side chains in κ-OR–JDTic and β_2-AR–carazolol complexes are shown by thin sticks with grey carbons. The graphics were prepared using the ICM molecular modelling package (Molsoft LLC).

reduction in affinity[30]. Similar to the observed JDTic conformation in the κ-OR–JDTic complex, a V-shaped conformation was found in the small molecule X-ray crystal structure of JDTic, which showed its amino groups coordinating a water molecule (Supplementary Fig. 7a). Although several rotatable bonds within the JDTic molecule allow for the sampling of different conformations (see Supplementary Fig. 7b) and facilitate the ligand passage through the narrow binding pocket entrance, the anchoring-type interaction of two amino groups with Asp 138$^{3.32}$ probably fixes the ligand in this characteristic V shape.

SAR studies have also underscored the importance of the distal hydroxyl groups on both the piperidine and isoquinoline moieties of JDTic, the removal of which did result in about a 100-fold reduction of affinity. A much smaller effect was observed upon methylation of these hydroxyls or their replacement by other polar groups[28]. These SAR results suggest the importance of water-mediated interactions between these two hydroxyl groups and the receptor. Indeed, although the crystal structure does not show direct hydrogen bonding with the receptor for both hydroxyl groups, there is clear electron density for several structured water molecules that mediate their polar interactions (Supplementary Fig. 6).

The κ-OR structure provides important clues for understanding the structural basis of the exceptional subtype selectivity of JDTic. Among many extensive contacts, JDTic interacts with four residues in the binding pocket that differ in other closely related opioid receptors, which are thought to contribute to the subtype selectivity of JDTic and other κ-OR-selective ligands[32] (human μ-OR and δ-OR amino acids are shown in parentheses, respectively): Val 108$^{2.53}$ (Ala and Ala), Val 118$^{2.63}$ (Asn and Lys), Ile 294$^{6.55}$ (Val and Val) and Tyr 312$^{7.35}$ (Trp and Leu) (Fig. 2b and Supplementary Fig. 8). Analysis of JDTic binding into κ-OR-based μ-OR and δ-OR homology models, as well as JDTic SAR results[17,28,30] (Supplementary Fig. 9), suggest that all described residues can contribute to the JDTic selectivity profile. Thus, changes in the Val 118$^{2.63}$ side chain, where larger hydrophilic residues Asn$^{2.63}$ and Lys$^{2.63}$ are found in the human μ-OR and δ-OR, respectively, are likely to introduce unfavourable contacts with JDTic. Additionally, changing Tyr 312$^{7.35}$ to the Trp$^{7.35}$ and Leu$^{7.35}$ residues found in the human μ-OR and δ-OR, respectively, is likely to result in the loss of an important polar interaction with the JDTic amide. The remaining two hydrophobic side-chain replacements, Val to Ala at position 2.53 and Ile to Val at position 6.55, may cause a reduction of the hydrophobic contact between JDTic and the receptor.

The isopropyl group of JDTic reaches deep into the orthosteric pocket to form a hydrophobic interaction with a conserved Trp 287$^{6.48}$ side chain, possibly having a critical role in the pharmacological properties of this ligand. Trp$^{6.48}$ is thought to be a key part of the activation mechanism in many class A GPCRs, including rhodopsin[26] and the A_{2A}AR[25], and similar hydrophobic contacts have been implicated in blocking activation-related conformational changes in the dark state visual rhodopsin by 11-*cis* retinal, and by inverse agonists in the A_{2A}AR and D3R.

Binding of κ-OR-selective morphinans

Prior mutagenesis and modelling studies suggested that many small-molecule opioid ligands can interact with the κ-OR, as well as with the μ-OR and δ-OR, by forming a salt bridge with the highly conserved Asp$^{3.32}$ (refs 33, 34). This is consistent with our mutagenesis studies (Supplementary Table 3) and flexible docking[35] of a series of morphine analogues, including selective κ-OR antagonists norbinaltorphimine (nor-BNI) and 5′-guanidinonaltrindole (GNTI) (Fig. 3 and Supplementary Fig. 10). To assess the compatibility of these bulky and rigid ligands with the observed κ-OR protein backbone conformation, we performed global energy optimizations of nor-BNI and GNTI in the binding cavity of κ-OR, keeping side chains of the binding pocket fully flexible. Multiple independent runs consistently resulted in low energy conformations with essentially identical poses and receptor contacts

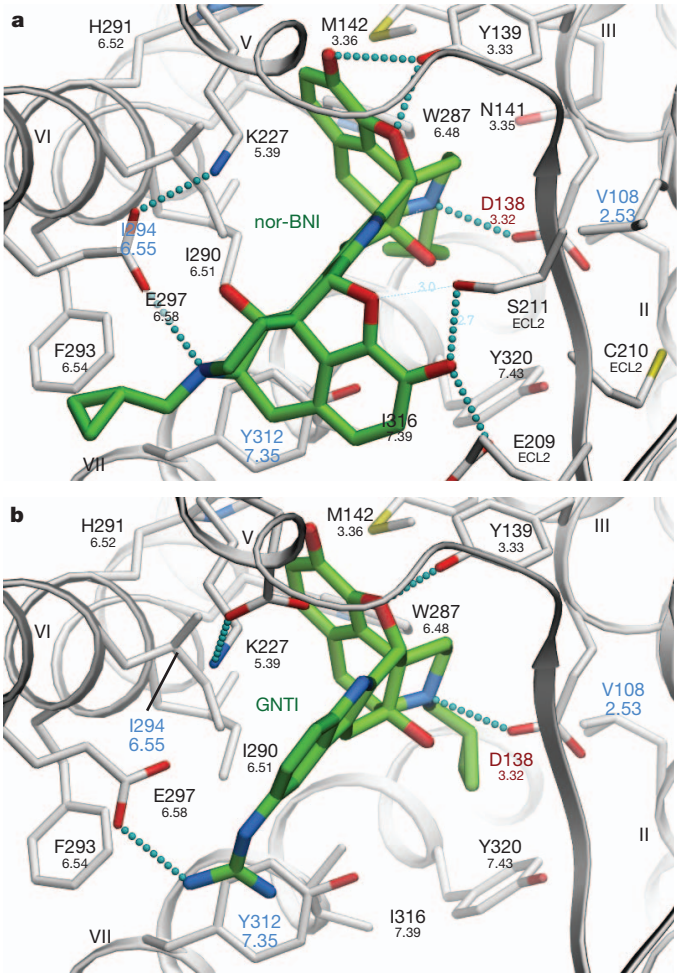

Figure 3 | Putative interaction modes of morphine-based high-affinity κ-OR-selective antagonists nor-BNI and GNTI. **a**, **b**, Interaction modes of nor-BNI (**a**) and GNTI (**b**). Ligands are depicted as capped sticks with green carbons, and contact side chains of the receptor within 4 Å from the ligand are shown with grey carbons. Key hydrogen bonds and salt bridges are indicated with small cyan spheres and residues unique to the κ-OR are labelled in blue. Residue Asp 138$^{3.32}$, which also shows critical impact on GNTI and nor-BNI binding in mutagenesis studies, is highlighted in red. Ballesteros–Weinstein residue numbers are shown under the κ-OR residue numbers. The graphics were prepared using the ICM molecular modelling package (Molsoft LLC).

for the common naltrexone moieties of both nor-BNI and GNTI (r.m.s.d. 0.85 Å). In addition to a highly complementary van der Waals interface, both compounds formed an amino group salt bridge to the Asp 138$^{3.32}$ side chain and a hydrogen bond to the Tyr 139$^{3.33}$ side chain, both of which are important anchoring points for binding of morphine-based ligands, as supported by previous mutagenesis studies[34].

Moreover, unlike JDTic, both nor-BNI and GNTI compounds have a second basic moiety located more than 10 Å away from the first amino group (the second morphine moiety in nor-BNI and the guanidine moiety in GNTI). In the predicted models of κ-OR–nor-BNI/GNTI complexes, these additional amino groups of both ligands form a salt bridge with Glu 297$^{6.58}$ located at the entrance to the ligand-binding pocket, which was previously characterized as a residue critical for subtype selectivity of κ-OR-selective morphinan derivatives[36]. This interaction is also supported by our mutagenesis results (Supplementary Table 3), where a Glu297Ala mutation induced a significant drop in both nor-BNI and GNTI binding affinity, but did not affect JDTic affinity. Hydrophobic interactions at the κ-OR-specific residue Ile 294 were also found for both nor-BNI and GNTI; consistent with our mutagenesis results (Supplementary

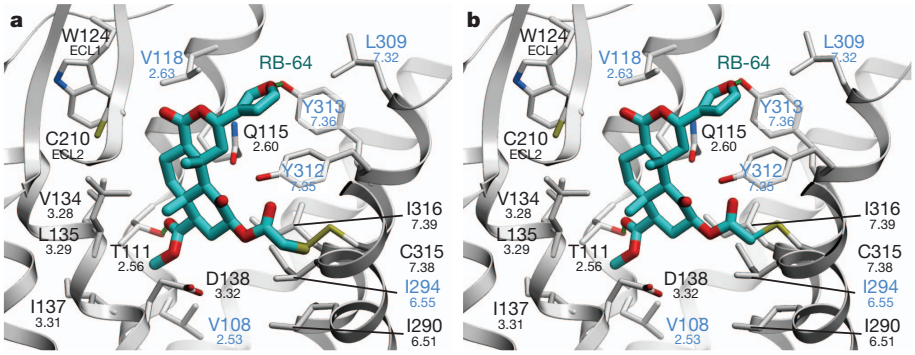

Figure 4 | Model of covalently bound RB-64. **a**, **b**, Putative binding mode of the RB-64 +463 AMU (**a**) and the RB-64 +431 AMU (**b**) adduct. Residues within 4 Å of the ligand are shown. Ligand, capped sticks/cyan carbons; κ-OR side chains, capped sticks; hydrogen bonds, small green spheres; κ-OR-unique residues are labelled in blue. Ballesteros–Weinstein residue numbers are shown under the κ-OR residue numbers. The graphics were prepared using the ICM molecular modelling package (Molsoft LLC).

Table 3) and suggesting that Ile 294 may also be important for developing human κ-OR-subtype-selective morphinan derivatives. Additional polar interactions with κ-OR-specific residues, Glu 209 and Ser 211 in ECL2, are found for nor-BNI, which may further enhance the κ-OR selectivity of this bulky ligand. Another side chain of the pocket, His $291^{6.52}$, which is involved in the highly conserved aromatic cluster around $Trp^{6.48}$ and thought to have a critical role in the receptor activation process[37], forms hydrophobic contacts with JDTic, nor-BNI and GNTI. His $291^{6.52}$ can be mutated to another aromatic residue, phenylalanine, without disrupting binding of these antagonists (Supplementary Table 3). The non-conservative $His291^{6.52}Lys$ mutation, however, abolished binding of all tested ligands, probably because of the disruption of the aromatic cluster induced by the lysine side chain. Interestingly, the cyclopropyl moiety of both nor-BNI and GNTI in these binding poses has the same position as the isopropyl moiety of JDTic, making hydrophobic contact with the conserved residue Trp $287^{6.48}$. This cyclopropyl moiety is generally implicated in conversion of opioid agonists into antagonists (for example, agonist oxymorphone into antagonist naltrexone), and this effect may be partially explained by a direct interaction with the Trp $287^{6.48}$ side chain.

Overall, these structure-based docking results support the 'message–address' model[38] for morphine-based ligands nor-BNI and GNTI[36], which points to Glu $297^{6.58}$ as a key side chain that controls κ-OR selectivity by anchoring the 'address' moieties of these compounds. The crystal structure of the κ-OR–JDTic complex (Figs 2 and 3), however, demonstrates that even without an 'address' interaction with Glu $297^{6.58}$, more than a 1,000-fold subtype-selectivity to κ-OR can be achieved for JDTic and some of its derivatives. Importantly, then, the message–address hypothesis does not uniformly apply to all κ-OR-selective antagonists.

Binding of salvinorins

SalA, a naturally occurring diterpene from the widely abused hallucinogenic plant *Salvia divinorum*, represents an exceedingly potent (half-maximum effective concentration (EC_{50}) = 1 nM) and selective κ-OR agonist (>1,000-fold)[15]. SalA is unique compared to other κ-OR ligands in that it lacks a charged or polar nitrogen atom to anchor it in the binding pocket. Extensive site-directed mutagenesis, substituted cysteine-accessibility mutagenesis (SCAM) and SAR studies on SalA and its analogues have been performed, indicating (among others) that the 2-acetoxy moiety interacts with Cys $315^{7.38}$ (ref. 39). Possible modes of interaction between the cysteine-reactive and ultra-potent agonist and SalA analogue 22-thiocyanatosalvinorin A (RB-64; K_i = 0.59 nM; EC_{50} = 0.077 nM)[39], and the human κ-OR structure were thus evaluated. Exposure of κ-OR to RB-64 produces irreversibly bound, wash-resistant adducts that are tethered to Cys $315^{7.38}$ (ref. 39). As the thiocyanate group contains two electrophilic centres, two distinct adducts may be formed, increasing the mass by either 463 or 431 AMU. Docking studies using GOLD[40] predict that the salvinorin 2-position can access Cys $315^{7.38}$ while maintaining many of the interactions implicated by site-directed mutagenesis for SalA, providing a possible mechanism for the formation of the κ-OR–RB-64 adduct (Fig. 4, Supplementary Tables 4 and 5, and Supplementary Figs 11 and 12). Additionally, the docking results serve as a model of the initial recognition process of SalA-related agonists of the human κ-OR in an inactive state, although additional studies will be needed to fully elucidate the nature of the SalA-induced activation mechanism.

Conclusions

The κ-OR–JDTic crystal structure has uncovered a combination of key features shared with chemokine and aminergic GPCRs along with unique structural details characteristic of the opioid subfamily. The human κ-OR was crystallized as a parallel dimer with contacts involving helices I, II and VIII. Although the existence of GPCR dimers *in vivo* and their physiological relevance remain highly debatable, several distinct potential dimer interfaces are starting to emerge from crystallographic and biochemical studies. Such multiple dimerization interfaces may serve to support different functional pathways, as well as to promote oligomeric assembly of GPCRs. Analysis of ligand–receptor interactions has revealed important molecular details of the exceptionally high affinity and subtype selectivity of JDTic, a small-molecule antagonist with a broad therapeutic potential. The elucidation of a large binding cavity with a multitude of potential anchoring points begins to explain both the broad structural diversity of drugs targeting the human κ-OR and differences in their receptor interaction modes, as supported by differential effects of various site-directed mutations on the binding properties of chemically diverse prototypic ligands. The human κ-OR structure provides a long anticipated molecular framework for understanding opioid drug action, and thereby affords valuable new opportunities for the structure-based discovery of new drugs with ideal pharmacological properties.

METHODS SUMMARY

κ-OR–T4L was expressed in *Spodoptera frugiperda* (Sf9) cells. Ligand-binding and functional assays were performed as described in Methods. Receptor–ligand complexes were solubilized from washed Sf9 membranes using 1% (w/v) *n*-dodecyl-*β*-D-maltopyranoside (DDM) and 0.2% (w/v) cholesteryl hemisuccinate (CHS), and purified by immobilized metal ion affinity chromatography (IMAC), followed by reverse IMAC after cleaving N-terminal Flag–10×His tags by His-tagged tobacco etch virus (TEV) protease. The purified protein solution was mixed with monoolein and cholesterol in a ratio of 40%:54%:6% (w/w) to form lipidic cubic phase (LCP) from which the receptor was crystallized. Crystals were grown at 20 °C in 45 nl protein-laden LCP boluses overlaid by 800 nl of precipitant solutions as described in Methods. Crystals were harvested from the LCP matrix and flash frozen in liquid nitrogen. X-ray diffraction data were collected on the 23ID-B/D beamline (GM/CA CAT) at the Advanced Photon Source, Argonne, using a 10 μm minibeam at a wavelength of 1.0330 Å. Data collection, processing, structure solution and refinement are described in Methods. Modelling of JDTic analogues and κ-OR-selective

morphine derivatives nor-BNI and GNTI was performed using ICM-Pro; SYBYL-X 1.3 and GOLD Suite 5.1 were used to model RB-64 complexes, as described in Methods.

Full Methods and any associated references are available in the online version of the paper at www.nature.com/nature.

Received 31 December 2011; accepted 10 February 2012.

Published online 21 March 2012.

1. Fredriksson, R., Lagerstrom, M. C., Lundin, L. G. & Schioth, H. B. The G-protein-coupled receptors in the human genome form five main families. Phylogenetic analysis, paralogon groups, and fingerprints. *Mol. Pharmacol.* **63,** 1256–1272 (2003).
2. Waldhoer, M., Bartlett, S. E. & Whistler, J. L. Opioid receptors. *Annu. Rev. Biochem.* **73,** 953–990 (2004).
3. Cherezov, V. *et al.* High-resolution crystal structure of an engineered human β_2-adrenergic G protein-coupled receptor. *Science* **318,** 1258–1265 (2007).
4. Jaakola, V. P. *et al.* The 2.6 angstrom crystal structure of a human A_{2A} adenosine receptor bound to an antagonist. *Science* **322,** 1211–1217 (2008).
5. Chien, E. Y. *et al.* Structure of the human dopamine D3 receptor in complex with a D2/D3 selective antagonist. *Science* **330,** 1091–1095 (2010).
6. Warne, T. *et al.* Structure of a β_1-adrenergic G-protein-coupled receptor. *Nature* **454,** 486–491 (2008).
7. Shimamura, T. *et al.* Structure of the human histamine H_1 receptor complex with doxepin. *Nature* **475,** 65–70 (2011).
8. Wu, B. *et al.* Structures of the CXCR4 chemokine GPCR with small-molecule and cyclic peptide antagonists. *Science* **330,** 1066–1071 (2010).
9. Rasmussen, S. G. *et al.* Crystal structure of the β_2 adrenergic receptor–Gs protein complex. *Nature* **477,** 549–555 (2011).
10. Katritch, V., Cherezov, V. & Stevens, R. C. Diversity and modularity of G protein-coupled receptor structures. *Trends Pharmacol. Sci.* **33,** 17–27 (2011).
11. Congreve, M., Langmead, C. J., Mason, J. S. & Marshall, F. H. Progress in structure based drug design for G protein-coupled receptors. *J. Med. Chem.* **54,** 4283–4311 (2011).
12. Kufareva, I., Rueda, M., Katritch, V., Stevens, R. C. & Abagyan, R. Status of GPCR modeling and docking as reflected by community-wide GPCR Dock 2010 assessment. *Structure* **19,** 1108–1126 (2011).
13. Martin, W. R., Eades, C. G., Thompson, J. A., Huppler, R. E. & Gilbert, P. E. The effects of morphine- and nalorphine- like drugs in the nondependent and morphine-dependent chronic spinal dog. *J. Pharmacol. Exp. Ther.* **197,** 517–532 (1976).
14. Carlezon, W. A. Jr, Beguin, C., Knoll, A. T. & Cohen, B. M. Kappa-opioid ligands in the study and treatment of mood disorders. *Pharmacol. Ther.* **123,** 334–343 (2009).
15. Roth, B. L. *et al.* Salvinorin A: a potent naturally occurring nonnitrogenous κ opioid selective agonist. *Proc. Natl Acad. Sci. USA* **99,** 11934–11939 (2002).
16. Walsh, S. L., Strain, E. C., Abreu, M. E. & Bigelow, G. E. Enadoline, a selective kappa opioid agonist: comparison with butorphanol and hydromorphone in humans. *Psychopharmacology* (*Berl.*) **157,** 151–162 (2001).
17. Thomas, J. B. *et al.* Identification of the first trans-(3*R*,4*R*)- dimethyl-4-(3-hydroxyphenyl)piperidine derivative to possess highly potent and selective opioid κ receptor antagonist activity. *J. Med. Chem.* **44,** 2687–2690 (2001).
18. Carroll, F. I. *et al.* Pharmacological properties of JDTic: a novel κ-opioid receptor antagonist. *Eur. J. Pharmacol.* **501,** 111–119 (2004).
19. Jackson, K. J., Carroll, F. I., Negus, S. S. & Damaj, M. I. Effect of the selective kappa-opioid receptor antagonist JDTic on nicotine antinociception, reward, and withdrawal in the mouse. *Psychopharmacology* (*Berl.*) **210,** 285–294 (2010).
20. Salom, D. *et al.* Crystal structure of a photoactivated deprotonated intermediate of rhodopsin. *Proc. Natl Acad. Sci. USA* **103,** 16123–16128 (2006).
21. Mancia, F., Assur, Z., Herman, A. G., Siegel, R. & Hendrickson, W. A. Ligand sensitivity in dimeric associations of the serotonin 5HT2c receptor. *EMBO Rep.* **9,** 363–369 (2008).
22. Wang, J. B., Johnson, P. S., Wu, J. M., Wang, W. F. & Uhl, G. R. Human κ opiate receptor second extracellular loop elevates dynorphin's affinity for human μ/κ chimeras. *J. Biol. Chem.* **269,** 25966–25969 (1994).
23. Ballesteros, J. A. & Weinstein, H. Integrated methods for the construction of three-dimensional models and computational probing of structure-function relations in G protein-coupled receptors. *Methods Neurosci.* **25,** 366–428 (1995).
24. Palczewski, K. *et al.* Crystal structure of rhodopsin: a G protein-coupled receptor. *Science* **289,** 739–745 (2000).
25. Xu, F. *et al.* Structure of an agonist-bound human A_{2A} adenosine receptor. *Science* **332,** 322–327 (2011).
26. Standfuss, J. *et al.* The structural basis of agonist-induced activation in constitutively active rhodopsin. *Nature* **471,** 656–660 (2011).
27. Subramanian, G., Paterlini, M. G., Larson, D. L., Portoghese, P. S. & Ferguson, D. M. Conformational analysis and automated receptor docking of selective arylacetamide-based κ-opioid agonists. *J. Med. Chem.* **41,** 4777–4789 (1998).
28. Cai, T. B. *et al.* Synthesis and *in vitro* opioid receptor functional antagonism of analogues of the selective kappa opioid receptor antagonist (3*R*)-7-hydroxy-*N*-((1*S*)-1-{[(3*R*,4*R*)-4-(3-hydroxyphenyl)-3,4-dimethyl-1-pipe ridinyl]methyl}-2-methylpropyl)-1,2,3,4-tetrahydro-3-isoquinolinecarboxamide (JDTic). *J. Med. Chem.* **51,** 1849–1860 (2008).
29. Thomas, J. B. *et al.* Importance of phenolic address groups in opioid kappa receptor selective antagonists. *J. Med. Chem.* **47,** 1070–1073 (2004).
30. Runyon, S. P. *et al.* Analogues of (3*R*)-7-hydroxy-*N*-[(1*S*)-1-{[(3*R*,4*R*)-4-(3-hydroxyphenyl)-3,4-dimethyl-1-pipe ridinyl]methyl}-2-methylpropyl)-1,2,3,4-tetrahydro-3-isoquinolinecarboxamide (JDTic). Synthesis and *in vitro* and *in vivo* opioid receptor antagonist activity. *J. Med. Chem.* **53,** 5290–5301 (2010).
31. Zimmerman, D. M., Nickander, R., Horng, J. S. & Wong, D. T. New structural concepts for narcotic antagonists defined in a 4-phenylpiperidine series. *Nature* **275,** 332–334 (1978).
32. Vortherms, T. A., Mosier, P. D., Westkaemper, R. B. & Roth, B. L. Differential helical orientations among related G protein-coupled receptors provide a novel mechanism for selectivity. Studies with salvinorin A and the κ-opioid receptor. *J. Biol. Chem.* **282,** 3146–3156 (2007).
33. Surratt, C. K. *et al.* -mu opiate receptor. Charged transmembrane domain amino acids are critical for agonist recognition and intrinsic activity. *J. Biol. Chem.* **269,** 20548–20553 (1994).
34. Befort, K. *et al.* The conserved aspartate residue in the third putative transmembrane domain of the delta-opioid receptor is not the anionic counterpart for cationic opiate binding but is a constituent of the receptor binding site. *Mol. Pharmacol.* **49,** 216–223 (1996).
35. Totrov, M. & Abagyan, R. Flexible protein-ligand docking by global energy optimization in internal coordinates. *Proteins* **29,** 215–220 (1997).
36. Metzger, T. G., Paterlini, M. G., Portoghese, P. S. & Ferguson, D. M. Application of the message-address concept to the docking of naltrexone and selective naltrexone-derived opioid antagonists into opioid receptor models. *Neurochem. Res.* **21,** 1287–1294 (1996).
37. Chen, S. *et al.* Mutation of a single TMVI residue, Phe^{282}, in the β_2-adrenergic receptor results in structurally distinct activated receptor conformations. *Biochemistry* **41,** 6045–6053 (2002).
38. Chavkin, C. & Goldstein, A. Specific receptor for the opioid peptide dynorphin: structure–activity relationships. *Proc. Natl Acad. Sci. USA* **78,** 6543–6547 (1981).
39. Yan, F. *et al.* Structure-based design, synthesis, and biochemical and pharmacological characterization of novel salvinorin A analogues as active state probes of the κ-opioid receptor. *Biochemistry* **48,** 6898–6908 (2009).
40. Verdonk, M. L., Cole, J. C., Hartshorn, M., Murray, C. W. & Taylor, R. Improved protein-ligand docking using GOLD. *Proteins* **52,** 609–623 (2003).

Supplementary Information is linked to the online version of the paper at www.nature.com/nature.

Acknowledgements This work was supported by PSI:Biology grant U54 GM094618 (V.K., V.C., R.C.S.) for biological studies and structure production, NIH Roadmap grant P50 GM073197 (V.C., R.C.S.) for technology development and R01 DA017624 (B.L.R., E.V., R.B.M., P.D.M.), R01 DA027170 (B.L.R.), the NIMH Psychoactive Drug Screening Program Contract (B.L.R., X.-P.H.), the Michael Hooker Distinguished Chair of Pharmacology (B.L.R.), and the NIH grant R01 DA009045 (F.I.C.). D.W. is supported by a Boehringer Ingelheim Fonds PhD Fellowship. The JDTic X-ray structure was determined by C. George at the Laboratory for the Structure of Matter, Naval Research Laboratory. We thank J. Velasquez for help on molecular biology; T. Trinh, K. Allin and M. Chu for help on baculovirus expression; V. Setola for help with functional activity assays; J. Evans for help acquiring compounds; the National Institute of Drug Abuse Drug Supply Program for supplying JDTic and other opioid ligands used in these studies; K. Kadyshevskaya for assistance with figure preparation; E. Abola for assistance with manuscript preparation; A. Walker for assistance with manuscript preparation; J. Smith, R. Fischetti and N. Sanishvili for assistance in the development and use of the minibeam and beamtime at GM/CA-CAT beamline 23-ID at the Advanced Photon Source, which is supported by National Cancer Institute grant Y1-CO-1020 and National Institute of General Medical Sciences grant Y1-GM-1104.

Author Contributions H.W. assisted with protein expression, optimized the constructs, purified and crystallized the receptor in LCP, optimized crystallization conditions, grew crystals for data collection, collected the data and processed diffraction data, and prepared the manuscript. D.W. assisted with protein expression, purified the receptor, performed the thermal stability assay and assisted with preparing the manuscript. M.M. assisted with protein expression, purified the receptor, tested the JDTic compound, and performed the thermal stability assay. V.K. performed nor-BNI/GNTI-receptor docking and prepared the manuscript. G.W.H. processed diffraction data, solved and refined the structure and assisted with preparing the manuscript. E.V. created the initial tagged human κ-OR constructs and E.V. and X.-P.H. performed the ligand-binding and site-directed mutagenesis studies. W.L. assisted with construct optimization and crystallization in LCP. A.A.T. refined the structure and assisted with preparing the manuscript. F.I.C. and S.W.M. provided JDTic crystal structure, performed conformational studies of JDTic, and assisted with preparing the manuscript. R.B.W. and P.D.M. performed RB-64-receptor docking and prepared the manuscript. V.C. assisted with the crystallization in LCP, processed diffraction data, refined the structure and prepared the manuscript. B.L.R. suggested the JDTic compound for structural studies, supervised the pharmacology and mutagenesis studies and prepared the manuscript. R.C.S. was responsible for the overall project strategy and management and led the manuscript preparation and writing.

Author Information The coordinates and structure factors have been deposited in the Protein Data Bank under accession code 4DJH. Reprints and permissions information is available at www.nature.com/reprints. The authors declare competing financial interests: details accompany the full-text HTML version of the paper at www.nature.com/nature. Readers are welcome to comment on the online version of this article at www.nature.com/nature. Correspondence and requests for materials should be addressed to R.C.S. (stevens@scripps.edu).

METHODS

Protein engineering for structural studies. Human κ-OR was engineered for structural studies by fusing lysozyme from T4 phage (T4L) into ICL3 (Gly 261–Arg 263) and further modified by N/C-terminal truncations (ΔGlu2–Ala42, ΔArg359–Val380) and a single point mutation Ile135$^{3.29}$Leu (see Supplementary Information). The resulting κ-OR–T4L construct was subsequently expressed in baculovirus-infected *Spodoptera frugiperda* (Sf9) insect cells.

Generation of κ-OR constructs for Sf9 expression. The human κ-OR (I135L) cDNA provided by the NIMH Psychoactive Drug Screening Program was cloned into a modified pFastBac1 vector (Invitrogen), designated as pFastBac1-833100, which contained an expression cassette with a haemagglutinin (HA) signal sequence followed by a Flag tag, a 10×His tag[3], and a TEV protease recognition site at the N terminus before the receptor sequence. Subcloning into the pFastBac1-833100 was achieved using PCR with primer pairs encoding restriction sites BamHI at the 5′ and HindIII at the 3′ termini of κ-OR wild type with subsequent ligation into the corresponding restriction sites found in the vector.

The κ-OR–T4L gene, based on the human κ-OR (I135L) and cysteine-free lysozyme from bacteriophage T4 (T4L C54T, C97A) sequences[41], included the following additional features: (1) residue Ser 262 at ICL3 of κ-OR was deleted by using standard QuickChange PCR; (2) Asn 2–Tyr 161 of T4L were inserted between Gly 261 and Arg 263 within the ICL3 region; and (3) N-terminal residues 2–42 and C-terminal residues 359–380 of κ-OR were truncated.

Expression and purification of κ-OR constructs. High-titre recombinant baculovirus ($>10^9$ viral particles per ml) was obtained using the Bac-to-Bac Baculovirus Expression System (Invitrogen) as previously described[5,8]. 25 μM of the antagonist naltrexone (NTX) and 5% Protein Boost Additive (PBA) were added to the system during expression. Cell suspensions were incubated for 4 days while shaking at 27 °C. Production of high-titre baculovirus stocks was performed as described before[5,8]. Sf9 cells at a cell density of $2–3 \times 10^6$ cells ml^{-1} were infected with P2 virus at a m.o.i. (multiplicity of infection) of 2. Cells were harvested by centrifugation at 48 h post-infection and stored at −80 °C until use.

Insect cell membranes were disrupted by thawing frozen cell pellets in a hypotonic buffer containing 10 mM HEPES, pH 7.5, 10 mM $MgCl_2$, 20 mM KCl and EDTA-free complete protease inhibitor cocktail tablets (Roche). Extensive washing of the raw membranes was performed by repeated centrifugation in the same hypotonic buffer (two to three times), and then in a high osmotic buffer containing 1.0 M NaCl, 10 mM HEPES, pH 7.5, 10 mM $MgCl_2$, 20 mM KCl and EDTA-free complete protease inhibitor cocktail tablets (three to four times), thereby separating soluble and membrane associated proteins from integral transmembrane proteins.

Washed membranes were resuspended into buffer containing 40 μM NTX, 2 mg ml^{-1} iodoacetamide, 150 mM NaCl and EDTA-free complete protease inhibitor cocktail tablets, and incubated at 4 °C for 1 h before solubilization. The membranes were then solubilized in 50 mM HEPES, pH 7.5, 150 mM NaCl, 1% (w/v) *n*-dodecyl-*β*-D-maltopyranoside (DDM, Anatrace), 0.2% (w/v) cholesteryl hemisuccinate (CHS, Sigma) and 20 μM NTX for 3 h at 4 °C. The supernatant was isolated by centrifugation at 160,000*g* for 40 min, and incubated in 30 mM buffered imidazole (pH 7.5), 1 M NaCl with TALON IMAC resin (Clontech) overnight at 4 °C. After binding, the resin was washed with 10 column volumes of Wash I Buffer (50 mM HEPES, pH 7.5, 800 mM NaCl, 10% (v/v) glycerol, 0.1% (w/v) DDM, 0.02% (w/v) CHS, 10 mM ATP, 10 mM $MgCl_2$ and 50 μM JDTic), followed by 6 column volumes of Wash II Buffer (50 mM HEPES, pH 7.5, 500 mM NaCl, 10% (v/v) glycerol, 0.05% (w/v) DDM, 0.01% (w/v) CHS, 50 mM imidazole and 50 μM JDTic). The protein was then eluted by 3 column volumes of Elution Buffer (50 mM HEPES, pH 7.5, 300 mM NaCl, 10% (v/v) glycerol, 0.03% (w/v) DDM, 0.006% (w/v) CHS, 250 mM imidazole and 50 μM JDTic). PD MiniTrap G-25 column (GE healthcare) was used to remove imidazole. The protein was then treated overnight with His-tagged AcTEV protease (Invitrogen) to cleave the N-terminal His-tag and Flag-tag. AcTEV protease and cleaved N-terminal fragment were removed by TALON IMAC resin incubation at 4 °C for 2 h for binding. The tag-less protein was collected as the TALON IMAC column flow-through. The protein was then concentrated to 40 mg ml^{-1} with a 100 kDa molecular weight cut-off Vivaspin centrifuge concentrator (GE healthcare). Protein purity and monodispersity were tested by SDS–PAGE and analytical size-exclusion chromatography (aSEC). Typically, the protein purity exceeded 95%, and the aSEC profile showed a single peak, indicative of receptor monodispersity.

Lipidic cubic phase crystallization. Protein samples of κ-OR in complex with JDTic were reconstituted into lipidic cubic phase (LCP) by mixing with molten lipid in a mechanical syringe mixer[42]. LCP crystallization trials were performed using an NT8-LCP crystallization robot (Formulatrix) as previously described[43]. 96-well glass sandwich plates (Marienfeld) were incubated and imaged at 20 °C using an automated incubator/imager (RockImager 1000, Formulatrix). Initial crystal hits were found from precipitant condition containing 100 mM sodium citrate pH 6.0, 30% (v/v) PEG400, 400 mM potassium nitrate. After extensive optimization, crystals of 30 μm × 10 μm × 5 μm to 60 μm × 20 μm × 10 μm size were obtained in 100 mM sodium citrate pH 5.8–6.4, 28–32% (v/v) PEG400, 350–450 mM potassium nitrate. Crystals were harvested directly from LCP matrix using MiTeGen micromounts and flash frozen in liquid nitrogen.

Data collection, structure solution and refinement. X-ray data were collected at the 23ID-B/D beamline (GM/CA CAT) at the Advanced Photon Source, Argonne, using a 10 μm minibeam at a wavelength of 1.0330 Å and a MarMosaic 300 CCD detector. Most crystals were invisible after flash freezing in liquid nitrogen, and a similar alignment and data-collection strategy was followed as previously described[44]. Among the several hundred crystal samples screened, most crystals diffracted to 2.8–3.5 Å resolution when exposed to 1–5 s of unattenuated beam using 1° oscillation. Data collection was limited to 5–10 frames per crystal, due to the fast onset of radiation damage in the microcrystals. Data were integrated, scaled and merged using HKL2000[45]. A 97% complete data set of κ-OR–T4L/JDTic (space group $P2_12_12_1$) at 2.9 Å resolution was obtained by merging data collected from 60 crystals. Initial phase information was obtained by molecular replacement with the program PHASER[46] using two independent search models of the polyalanine seven-transmembrane α-helices of CXCR4–IT1t (PDB accession 3ODU) and ensemble T4L models of β_2-AR–T4L (PDB accession 2RH1), A_{2A}AR–T4L (PDB accession 3EML), CXCR4–T4L (PDB accession 3ODU), D3R–T4L (PDB accession 3PBL) and H_1R–T4L (PDB accession 3RZE). Electron density refinement was performed with REFMAC5[47], autoBUSTER[48], and PHENIX[49] followed by manual examination and rebuilding of the refined coordinates in the program COOT[50] using both $|2F_o| - |F_c|$ and $|F_o| - |F_c|$ maps, as well as omit maps. The final model includes 287 residues of A chain (Ser 55–Gly 261, Arg 263–Ser 301, Ala 307–Pro 347) and 288 residues of B chain (Ser 55–Gly 261, Arg 263–Gly 300, Ser 305–Pro 347) of the κ-OR, and residues Asn 2–Tyr 161 of both A and B chains of T4L.

Ligand-binding assay. Membrane preparations, radioligand binding assays using ^{3}H-diprenorphine and data analyses were performed as previously described[39].

Modelling of high-affinity analogues of JDTic and morphine. Docking of high-affinity κ-OR-specific ligands was performed using an all-atom flexible receptor docking algorithm in ICM-Pro (MolSoft LLC) molecular modelling package as described previously[35]. Internal coordinate (torsion) movements were allowed in the side chains of the binding pocket, defined as residues within 10 Å distance of JDTic in the crystal structure. Other side chains and the backbone of the protein were kept as in the crystal structure. An initial conformation for each of the ligands was generated by Cartesian optimization of the ligand model in Merck Molecular Force Field. Docking was performed by placing the ligand in a random position within 5 Å from the entrance to the binding pocket and global conformational energy optimization of the complex[39,40]. To facilitate side-chain rotamer switches in flexible κ-OR models, the first 10^6 steps of the Monte Carlo (MC) procedure used 'soft' van der Waals potentials and high MC temperature, followed by another 10^6 steps with 'exact' van der Waals method and gradually decreasing temperature. A harmonic 'distance restraint' applied between an amino group of the ligand and carboxyl of Asp 138 side chain in the initial 10^6 steps was removed in the final 10^6 steps. At least 10 independent runs of the docking procedure were performed for each κ-OR ligand. The docking results were considered 'consistent' when at least 80% of the individual runs resulted in conformations clustered within a r.m.s.d. of <1 Å to the overall best energy pose of the ligand. All calculations were performed on a 12-core Linux workstation.

Modelling of RB-64. Modelling of RB-64 was performed using SYBYL-X 1.3 (Tripos) and GOLD 5.1 (Cambridge Crystallographic Data Centre)[40]. Default parameters were used except where noted. The structures of RB-64 and its κ-OR complexes were energy minimized using the Tripos Force Field (Gasteiger–Hückel charges, distance-dependent dielectric constant $\varepsilon = 4$, non-bonded interaction cut-off = 8 Å, energy gradient termination = 0.05 kcal/(mol × Å)). The κ-OR C315$^{7.38}$ χ_1 torsion angle was modified ($\chi_1 = +60.0°$), orienting the sulfhydryl group towards the binding cavity. A docking distance constraint was used (C315 SG atom to thiocyanate sulphur atom distance, 2.0–6.0 Å; spring constant = 5.0). The Q115$^{2.60}$, D138$^{3.32}$, I290$^{6.51}$, I294$^{6.55}$, Y313$^{7.36}$ and I316$^{7.39}$ side chains were allowed to flex via rotamer library. The GoldScore fitness function was used with early termination disabled for 30 genetic algorithm runs. Poses were selected based on their GoldScore and ability to explain the relevant observed biochemical data. Stereochemical quality was assessed using PROCHECK.

41. Rosenbaum, D. M. *et al.* GPCR engineering yields high-resolution structural insights into β_2-adrenergic receptor function. *Science* **318,** 1266–1273 (2007).

42. Caffrey, M. & Cherezov, V. Crystallizing membrane proteins using lipidic mesophases. *Nature Protocols* **4,** 706–731 (2009).
43. Cherezov, V., Peddi, A., Muthusubramaniam, L., Zheng, Y. F. & Caffrey, M. A robotic system for crystallizing membrane and soluble proteins in lipidic mesophases. *Acta Crystallogr. D* **60,** 1795–1807 (2004).
44. Cherezov, V. *et al.* Rastering strategy for screening and centring of microcrystal samples of human membrane proteins with a sub-10 μm size X-ray synchrotron beam. *J. R. Soc. Interface* **6** (Suppl. 5), S587–S597 (2009).
45. Otwinowski, Z. & Minor, W. Processing of X-ray diffraction data collected in oscillation mode. *Methods Enzymol.* **276,** 307–326 (1997).
46. McCoy, A. J. *et al.* Phaser crystallographic software. *J. Appl. Cryst.* **40,** 658–674 (2007).
47. Murshudov, G. N., Vagin, A. A. & Dodson, E. J. Refinement of macromolecular structures by the maximum-likelihood method. *Acta Crystallogr. D* **53,** 240–255 (1997).
48. Bricogne, G, *et al.* BUSTER v. 2.8.0 (Global Phasing, 2009).
49. Adams, P. D, *et al.* PHENIX: a comprehensive Python-based system for macromolecular structure solution. *Acta Crystallogr. D* **66,** 213–221 (2010).
50. Emsley, P., Lohkamp, B., Scott, W. G. & Cowtan, K. Features and development of Coot. *Acta Crystallogr. D* **66,** 486–501 (2010).